

This article was downloaded by:

On: 25 January 2011

Access details: *Access Details: Free Access*

Publisher *Taylor & Francis*

Informa Ltd Registered in England and Wales Registered Number: 1072954 Registered office: Mortimer House, 37-41 Mortimer Street, London W1T 3JH, UK



Separation Science and Technology

Publication details, including instructions for authors and subscription information:

<http://www.informaworld.com/smpp/title~content=t713708471>

Fine Bubble Aeration. Mathematical Modeling of Time-Dependent Operation

David J. Wilson^a

^a DEPARTMENT OF CHEMISTRY, VANDERBILT UNIVERSITY, NASHVILLE, TENNESSEE

To cite this Article Wilson, David J.(1988) 'Fine Bubble Aeration. Mathematical Modeling of Time-Dependent Operation', Separation Science and Technology, 23: 14, 2211 – 2230

To link to this Article: DOI: 10.1080/01496398808058451

URL: <http://dx.doi.org/10.1080/01496398808058451>

PLEASE SCROLL DOWN FOR ARTICLE

Full terms and conditions of use: <http://www.informaworld.com/terms-and-conditions-of-access.pdf>

This article may be used for research, teaching and private study purposes. Any substantial or systematic reproduction, re-distribution, re-selling, loan or sub-licensing, systematic supply or distribution in any form to anyone is expressly forbidden.

The publisher does not give any warranty express or implied or make any representation that the contents will be complete or accurate or up to date. The accuracy of any instructions, formulae and drug doses should be independently verified with primary sources. The publisher shall not be liable for any loss, actions, claims, proceedings, demand or costs or damages whatsoever or howsoever caused arising directly or indirectly in connection with or arising out of the use of this material.

Fine Bubble Aeration. Mathematical Modeling of Time-Dependent Operation

DAVID J. WILSON

DEPARTMENT OF CHEMISTRY
VANDERBILT UNIVERSITY
NASHVILLE, TENNESSEE 37235

Abstract

The operation of fine bubble aeration columns in the time-dependent mode is modeled. The kinetics of mass transfer between the solution and the rising bubbles is included by means of a time-constant approach. The magnitude of Δt is limited by the requirement that $u_w \cdot \Delta t / \Delta x$ be less than 1 (u_w is the linear velocity of the aqueous phase); the magnitudes of the mass transfer time constant and the rise velocity of the bubbles do not affect the maximum value of Δt which can be used. The time constant for mass transfer is the reciprocal of the least positive eigenvalue of a suitably chosen diffusion problem. The effects of influent flow rate, number of compartments into which the column is partitioned, bubble boundary layer thickness, and Henry's constant for the volatile solute are examined. Transient effects associated with startup and with concentration pulses in the influent are studied.

INTRODUCTION

Removal of volatile materials from water by fine bubble aeration has been treated in a number of standard references (1-3, for example); these steady-state models are very useful for the engineer designing an aeration facility for the treatment of influent streams having relatively constant flow rates and compositions. In the treatment of wastewaters, however, one is typically confronted with influent streams which are highly variable in both flow rate and composition. One then has the choice of 1) overdesigning the aeration column to handle the largest transient load on the assumption that this is a steady-state loading, 2) installing an

equalization tank to smooth out the loading to a set of values which make use of a steady-state model a reasonable approximation, or 3) utilizing a time-dependent model, together with information about the time dependences of the influent flow rate and concentration. This last method permits one to make use of the ability of the aeration column itself to buffer transient overloadings, and should permit some economies in the design of the facility.

Here we present a model of fine bubble aeration which allows one to examine the effect of time-dependent loading and which is suitable for use on commonly available microcomputers, such as the IBM PC and its compatibles. We first develop an equilibrium model for one-stage aeration, by way of introduction. This is then modified to take account of mass transport kinetics by means of a time constant approach. This, in turn, is then elaborated into a multistage model suitable for use with tall, baffled columns. The magnitude of the time constant for mass transport between the solution and the rising bubbles is then estimated. Lastly, we examine the results of the theory, illustrating how these depend on the values of the parameters used to describe the column and its operation.

EQUILIBRIUM MODEL, SINGLE-STAGE BUBBLE AERATION

The system being analyzed is pictured in Fig. 1. Let

$m(t)$ = mass of solute at time t in the solution being treated, g

V_1 = volume of solution being treated, mL

v_a = air flow rate, mL/s, at 1 atm and ambient temperature

c_1 = solute concentration in the solution, g/mL

c_a = solute concentration in the vapor phase in equilibrium with the solution, gm/mL

K_H = Henry's constant for the solute, defined by $c_a = K_H c_1$

A convenient formula for estimating Henry's constants is

$$K_H = \frac{1.603 \times 10^{-3} \cdot (\text{MW}) \cdot P^\circ(T)}{T \cdot c_s} \quad (1)$$

where (MW) = solute molecular weight, g/mol

$P^\circ(T)$ = solute vapor pressure at temperature T , °K, torr

c_s = solute solubility in water at temperature T , g/100 mL

Solubilities and vapor pressures depend markedly on temperature. If

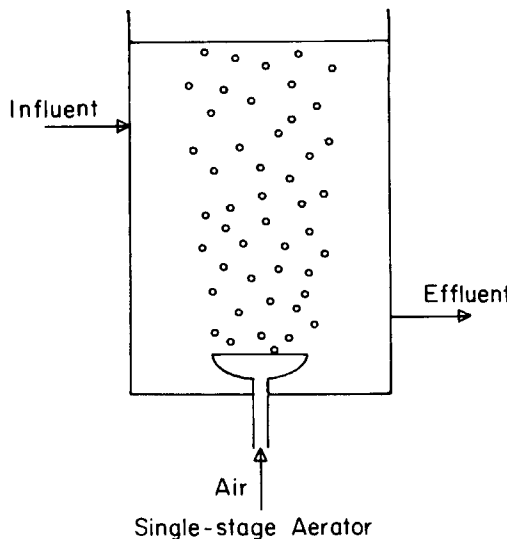


FIG. 1. Single-stage fine bubble aeration column.

data at the desired temperature are not available, a plot of $c_s(T)$ versus T or of $\log_{10} c_s(T)$ versus $1/T$ may be used to obtain c_s at the desired temperature. Vapor pressures are best estimated by a plot of $\log_{10} P^\circ(T)$ versus $1/T$, which is nearly linear.

The solute concentration and mass in the one-stage aerator under consideration are related by

$$c_1 V_1 = m \quad (2)$$

The amount of solute lost during a time interval dt is given by

$$\begin{aligned} -dm &= v_a c_a dt \\ &= v_a K_H c_1 dt \end{aligned} \quad (3)$$

Substitution from Eq. (2) then yields

$$\frac{dm}{m} = \frac{K_H v_a}{V_1} dt \quad (4)$$

from which

$$m(t) = m_0 \exp(-K_H v_a t / V_1) \quad (5)$$

or

$$c(t) = c_0 \exp(-K_H v_a t / V_1) \quad (6)$$

For a continuous flow apparatus operating in steady-state conditions, mass balance yields

$$v_{\text{infl}} c_{\text{infl}} = v_{\text{infl}} c_{\text{eff}} + v_a c_a \quad (7)$$

where v_{infl} = influent (and effluent) flow rate

c_{infl} = influent solute concentration

c_{eff} = effluent solute concentration

Equation (7) and Henry's law yield an expression for the effluent concentration,

$$c_{\text{eff}} = \frac{c_{\text{infl}}}{1 + v_a K_H / v_{\text{infl}}} \quad (8)$$

If a continuous-flow aerator is not operating in steady state, mass balance yields

$$V_1(t) \frac{dc_{\text{eff}}}{dt} = -(v_{\text{infl}} + v_a K_H) c_{\text{eff}} + v_{\text{infl}} c_{\text{infl}} \quad (9)$$

The flow rates of air (v_a) and water and the influent solute concentration may vary with time. $V_1(t)$, the volume of liquid in the aerator, is given by

$$V_1(t) = V_1(0) + \int_0^t (v_{\text{infl}} - v_{\text{eff}}) dt \quad (10)$$

where v_{eff} = effluent flow rate.

If $v_{\text{infl}} = v_{\text{eff}} = \text{constant}$ and v_a and c_{infl} are also held constant, the solution to Eq. (9) is given by

$$c_{\text{eff}}(t) = \left[c_{\text{eff}}(0) - \frac{v_{\text{infl}} c_{\text{infl}}}{v_{\text{infl}} + v_a K_H} \right] \exp \left[-\frac{v_{\text{infl}} + v_a K_H}{V_1} t \right] + \frac{v_{\text{infl}} c_{\text{infl}}}{v_{\text{infl}} + v_a K_H} \quad (11)$$

We see that the time constant governing the approach of the aerator to a steady state is given by

$$\tau_{ss} = \frac{V_1}{v_{\text{infl}} + v_a K_H} \quad (12)$$

EFFECT OF MASS TRANSPORT KINETICS ON THE OPERATION OF A SINGLE-STATE FINE BUBBLE AERATOR

Here we shall assume a first-order approach to equilibrium by a bubble rising through the aerator. The mass of solute $\mu(t)$ in a single bubble of radius a which is rising through the aerator is assumed to be determined by

$$\frac{d\mu}{dt} = k \cdot 4\pi a^2 \frac{(c_1 - c_a/K_H)}{b - a} \quad (13)$$

where $b - a$ = boundary layer thickness, cm

c_1 = solute concentration in the bulk liquid, g/mL

k = mass transfer rate coefficient, cm^2/s , to be calculated later

c_a = solute vapor concentration in the bubble

Noting that

$$\mu = \frac{4}{3} \pi a^3 c_a(t) \quad (14)$$

allows one to rewrite Eq. (13) as

$$\frac{dc_a}{dt} + \frac{3k}{a(b - a)K_H} c_a = \frac{3kc_1}{a(b - a)} \quad (15)$$

The solution to this equation yields

$$c_a(t) = c_1 K_H \left[1 - \exp \left(\frac{-3kt}{a(b - a)K_H} \right) \right] \quad (16)$$

or

$$\mu(t) = \frac{4\pi a^3}{3} c_1 K_H \left[1 - \exp \left(\frac{-3kt}{a(b - a)K_H} \right) \right]$$

If n bubbles per second are passing through the apparatus, then the mass of solute removed by aeration during a time interval dt is given by

$$-dm = n \cdot \frac{4\pi a^3}{3} K_H c_1 \left[1 - \exp \left(\frac{-3k\tau'}{a(b-a)K_H} \right) \right] dt \quad (17)$$

where τ' = transit time of a bubble through the liquid in the aerator.

Now,

$$n \cdot \frac{4\pi a^3}{3} = v_a \quad (18)$$

the air flow rate, and $c_1 = m/V_1$, which yields

$$dm = - \frac{v_a K_H}{V_1} \left[1 - \exp \left(\frac{-3k\tau'}{a(b-a)K_H} \right) \right] m dt \quad (19)$$

This yields the same results as we obtained for the local equilibrium model if we replace K_H by

$$K'_H = K_H \left[1 - \exp \left(\frac{-3k\tau'}{a(b-a)K_H} \right) \right] \quad (20)$$

We next estimate the bubble transit time τ' . The rise velocity of a bubble with respect to the surrounding fluid can be calculated over a range of Reynolds numbers from 0 to 10^4 from Eq. (21), modified from Fair, Geyer, and Okun (4).

$$u = \frac{2g\rho r_b^2}{9\eta} \left[1 + \frac{1}{4} \left(\frac{\rho r_b u}{2\eta} \right)^{1/2} + \frac{0.34\rho r_b u}{12\eta} \right]^{-1} \quad (21)$$

where g = gravitational constant, 980 cm/s²

ρ = fluid density, g/cm³

r_b = bubble radius, cm

η = viscosity, P

This equation is solved iteratively for the bubble rise velocity relative to the surrounding liquid, u .

The bubble rise velocity with respect to the aeration column, u_1 , is then obtained as follows. The volume of air in the column is given by

$$V_{\text{air}} = \frac{v_a}{u_1} L \quad (22)$$

where L is the height of the water column (cm). The volume of water in the column is

$$V_w = \pi(r_c)^2 L - v_a L / u_1 \quad (23)$$

where r_c is the column radius (cm). The linear velocity downward of the water in the column is

$$u_w = \frac{v_w}{\pi r_c^2 - v_a / u_1} \quad (24)$$

where v_w is the volumetric flow rate of the water. Now

$$u_1 = u - u_w \quad (25)$$

gives the bubble velocity relative to the apparatus. Substituting this into Eq. (24) yields

$$u_w = \frac{v_w}{\pi r_c^2 - v_a / (u - u_w)} \quad (26)$$

which can be rearranged to give a quadratic in u_w , the desired solution to which is

$$u_w = \left[\left(u - \frac{v_a}{\pi r_c^2} \right) - \left\{ \left(u - \frac{v_a}{\pi r_c^2} \right)^2 - \frac{4v_w}{\pi r_c^2} \right\}^{1/2} \right] / 2 \quad (27)$$

The rise velocity of the bubble relative to the apparatus is obtained by substituting this result into Eq. (25). The contact time of a bubble with the aqueous phase is then given by

$$\tau' = L / u_1 \quad (28)$$

This should be regarded as an upper bound, since the bubbles rising from the bottom of the column generally induce eddies and turbulence in the liquid which lead to rising currents in the column where the bubbles are most numerous. Because of this uncertainty, one is probably justified in approximating u_1 by u in Eq. (28).

MULTISTAGE MODEL FOR AERATION COLUMNS

If the aeration column is long and axial dispersion is controlled by baffling, use of a multistage model may be warranted. The model is illustrated in Fig. 2. We shall carry out the calculation in two steps. First, the increase in solute mass of a single bubble as it moves across the *i*th compartment representing the column is calculated under the assumption that the solute concentration in the bulk liquid can be regarded as constant during this short time interval. Second, this result is used in constructing the differential equations describing the changes in bulk liquid solute concentrations in the compartments used to model the column.

Let L = column length, cm

r_c = column radius, cm

a = mean bubble radius, cm

c_{infl} = influent solute concentration, g/mL

c_i^l = solute concentration in the liquid phase in the *i*th compartment, g/mL

c_i^a = solute concentration in the vapor phase at the top of the *i*th compartment, gm/mL

N = number of compartments into which the column is partitioned

$\Delta L = L/N$, the thickness of one compartment, cm

K_H = Henry's constant, dimensionless

k = mass transfer rate coefficient, cm^2/s

v_a = volumetric air flow rate, mL/s

v_w = volumetric water flow rate, mL/s

u = bubble rise velocity relative to aqueous phase, cm/s

Let us focus on a single bubble rising through the *i*th compartment. The mass of solute in the bubble is then determined by an equation similar to Eq. (15),

$$\frac{d\mu}{dt} = 4\pi a^2 k \frac{(c_i^l - c_i^a/K_H)}{b - a} \quad (29)$$

This integrates to give

$$\mu(t) = \left[\mu(0) - K_H c_i^l \cdot \frac{4\pi a^3}{3} \right] \exp \left(\frac{-3kt}{a(b - a)K_H} \right) + K_H c_i^l \cdot \frac{4\pi a^3}{3} \quad (30)$$

The transit time of a bubble across the *i*th compartment is given by

$$\tau' = \Delta L/u_1 \quad (31)$$

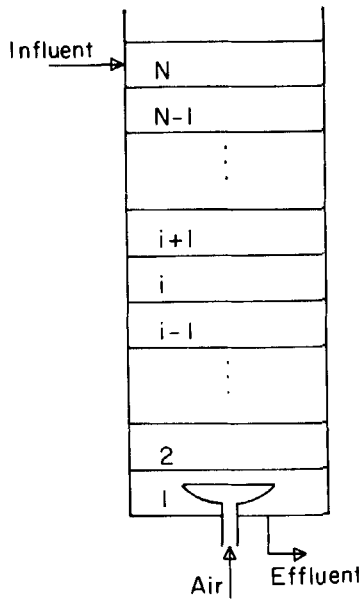


FIG. 2. Multistage aeration column.

where u_1 , the rise velocity of a bubble relative to the lab, is given by Eqs. (25) and (27). An approximation which is good at low water and air flow rates is

$$u_1 = u - \frac{v_w}{\pi r_c^2} \quad (32)$$

where u is calculated from Eq. (21).

The initial value of μ as the bubble crosses from the $(i-1)$ th to the i th compartment is defined as μ_{i-1} . The final value, as the bubble leaves the i th compartment, is taken as μ_i .

$$\begin{aligned} \mu_i = & \left[\mu_{i-1} - \frac{4\pi a^3}{3} K_H c_i^l \right] \exp \left(\frac{-3k\tau'}{a(b-a)K_H} \right) \\ & + \frac{4\pi a^3}{3} K_H c_i^l, \quad i = 1, 2, \dots, N \end{aligned} \quad (33)$$

$$\mu_0 = 0 \quad (34)$$

The increase in solute carried by the bubble resulting from its movement across the i th compartment is then given by $\mu_i - \mu_{i-1}$; this is the amount of solute in the i th compartment. The volume of liquid in the i th compartment is given by

$$V_i = (\pi r_c^2 - v_a/u_i) \Delta L \quad (35)$$

where u_i is calculated from Eqs. (25) and (27). Then

$$c_i^l = m_i/V_i \quad (36)$$

gives the concentration in the i th compartment. A solute material balance on this compartment gives

$$\frac{dm_i}{dt} = v_w(c_{i+1}^l - c_i^l) - \frac{3v_a}{4\pi a^3} (\mu_i - \mu_{i-1}) \quad (37)$$

The first term on the right-hand side of Eq. (37) represents simple advection of the liquid. The second term represents the removal of solute from the i th compartment in the vapor phase.

We then replace m_i in Eq. (37) by means of Eq. (36), obtaining

$$\frac{dc_i^l}{dt} = \frac{v_w}{V_i} (c_{i+1}^l - c_i^l) - \frac{3v_a}{4\pi a^3 V_i} (\mu_i - \mu_{i-1}), \quad i = 2, 3, \dots, N-1 \quad (38)$$

$$\frac{dc_N^l}{dt} = \frac{v_w}{V_i} (c_{\text{infl}} - c_N^l) - \frac{3v_a(\mu_N - \mu_{N-1})}{4\pi a^3 V_i} \quad (39)$$

$$\frac{dc_1^l}{dt} = \frac{v_w}{V_i} (c_2^l - c_1^l) - \frac{3v_a \mu_1}{4\pi a^3 V_i} \quad (40)$$

The simulation of a run is done as follows. Initial concentrations are selected—such as $c_{i1} = c_{\text{infl}}$ or $c_i^l = 0$. The μ_i are then calculated recursively from Eqs. (33) and (34). These are then used in Eqs. (38)–(40) to calculate the dc_i^l/dt values. These are used to numerically integrate the differential equations to obtain the values of the c_i^l at $t = \Delta t$. These values are in turn used to calculate the new values (at $t = \Delta t$) of the μ_i , and the process is repeated. A predictor-corrector method described by Ralston and Wilf (5)

provides an accurate, easily coded, and fast method for integrating Eqs. (38)–(40) forward in time.

Relatively large values of the time increment Δt can be used in this model, since Δt is limited by neither the time constant associated with mass transfer into a bubble nor with the transit time of a bubble across one of the compartments representing the column. An upper bound of Δt is given by the requirement that Δt be less than $\Delta L/u_w$, where u_w is the linear velocity of the water in the column. This is a much more generous criterion than those which come from mass transfer rate or bubble transit time.

Steady-state models are generally preferred over time-dependent representations because the former require less computation. The present model, however, runs to steady state in a couple of minutes or less under fairly typical conditions when a Zenith 150 microcomputer running compiled BASICA at 4.77 MHz is used.

ESTIMATION OF THE MASS TRANSPORT TIME CONSTANT

In this section we calculate an estimate of the time constant for diffusion of volatile solute from the bulk liquid through the boundary layer of liquid around the bubble into the bubble. Since gas-phase diffusion constants are very much larger than liquid-phase diffusion constants, we assume that complete mixing within the bubble itself is instantaneous on our time scale. We follow Huang et al. (6).

The diffusion equation appropriate for a problem with spherical symmetry is

$$\frac{\partial c}{\partial t} = \frac{D}{r^2} \frac{\partial}{\partial r} \left(r^2 \frac{\partial c}{\partial r} \right), \quad a \leq r \leq b \quad (41)$$

where D = solute diffusion constant in water, cm^2/s

c = solute concentration in the solution at time t and distance r from the center of the bubble

a = bubble radius

b = radius of bubble plus its boundary layer

Equation (41) is readily solved by separation of variables; a general solution is

$$c(r,t) = \frac{A_0}{r} + B_0 + \frac{1}{r} \sum_{\lambda} \left[A_{\lambda} \sin \sqrt{\frac{\lambda}{D}} r + B_{\lambda} \cos \sqrt{\frac{\lambda}{D}} r \right] e^{-\lambda t} \quad (42)$$

Mass balance considerations yield

$$\frac{dm_b}{dt} = 4\pi a^2 D \frac{\partial c}{\partial r}, \quad r = a \quad (43)$$

where m_b is the mass of solute in the bubble. Now

$$m_b = \frac{4\pi a^3}{3} K_H c(a, t) \quad (44)$$

from Henry's law, so

$$\frac{dm_b}{dt} = \frac{4\pi a^3}{3} K_H \frac{\partial c}{\partial t}(a, t) \quad (45)$$

Equations (43) and (45) then give

$$\frac{\partial c}{\partial t}(a, t) = \frac{3D}{a K_H} \frac{\partial c}{\partial r}(a, t) \quad (46)$$

This provides one of the problem's boundary conditions. The other, at $r = b$, is simply

$$c(b, t) = c_\infty \quad (47)$$

where c_∞ is the bulk solute concentration.

One then substitutes Eq. (42) into Eqs. (46) and (47) to get a pair of linear homogeneous equations for A_λ and B_λ ; the existence of nonzero values for these requires that the determinant of the coefficients of this system vanish. The linear equations are

$$\frac{A_\lambda}{b} \sin \sqrt{\frac{\lambda}{D}} b + \frac{B_\lambda}{b} \cos \sqrt{\frac{\lambda}{D}} b = 0 \quad (48)$$

and

$$A_\lambda \left\{ \frac{1}{a^2} \sin \sqrt{\frac{\lambda}{D}} a - \frac{\sqrt{\frac{\lambda}{D}}}{a} \cos \sqrt{\frac{\lambda}{D}} a - \frac{3D\lambda}{K_H a^2} \sin \sqrt{\frac{\lambda}{D}} a \right\}$$

$$+ B_\lambda \left\{ \frac{1}{a^2} \cos \sqrt{\frac{\lambda}{D}} a + \frac{\sqrt{\frac{\lambda}{D}}}{a} \sin \sqrt{\frac{\lambda}{D}} a - \frac{3D\lambda}{K_H a^2} \cos \sqrt{\frac{\lambda}{D}} a \right\} = 0 \quad (49)$$

Setting the determinant of this system to zero yields a remarkably simple result for the eigenvalue equation,

$$\tan \sqrt{\frac{\lambda}{D}} (b - a) + \frac{\sqrt{\frac{\lambda}{D}} a}{1 - \frac{K_H a^2}{3} \frac{\lambda}{D}} = 0 \quad (50)$$

It is evident from Eq. (50) that the λ_i are proportional to D , as expected. We take $1/\lambda_1$ as the time constant for mass transfer, where λ_1 is the lowest nonzero root of Eq. (50). The relationship between k , the mass transfer rate coefficient, and λ_1 is obtained by setting the time constant in Eq. (16) equal to λ_1 , which yields

$$k = \frac{a(b - a)K_H}{3} \lambda_1 \quad (51)$$

RESULTS OF THE MODEL

Aeration columns show a fairly sharply defined breakthrough on overload. This is seen in Fig. 3, in which effluent concentrations are plotted versus time. The sharpness of the break increases with increasing number of compartments; in this figure runs are shown for columns represented by 5 and 25 compartments. (We note that these compartments are not equivalent to theoretical transfer units or theoretical plates; that model assumes local equilibrium.) The influent flow rates range from 0.25 to 4.0 mL/s. These effluent concentrations are all for steady-state conditions.

When columns are not overloaded, the number of compartments has a very marked effect on column performance, as shown in Fig. 4. Here three sets of identical runs (with influent flow rates of 2.25, 2.0, and 1.75 mL/s) are shown for columns represented by 1, 2, 3, 4, 5, 10, 20, and 25 compartments. Obviously one is well-advised to reduce axial dispersion as much as possible in aeration columns if one is seeking maximum removal efficiencies.

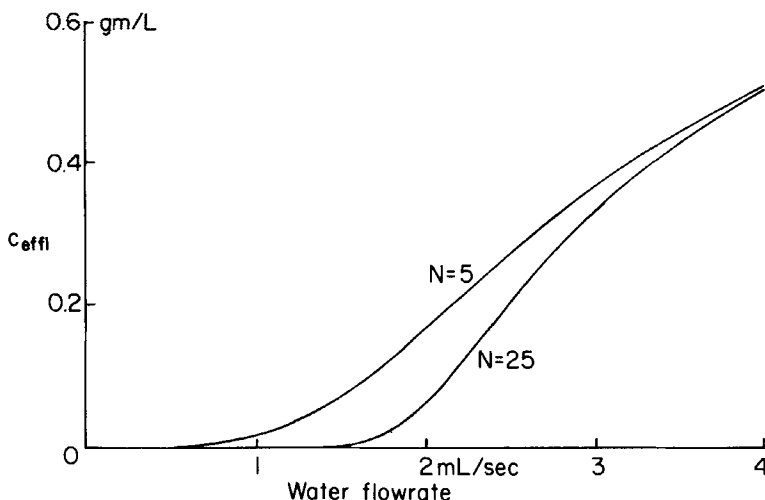


FIG. 3. Effect of water flow rate on effluent solute concentration. Column height = 100 cm; column radius = 5 cm; Henry's constant = 0.2 (dimensionless); air flow rate = 10 mL/s; bubble radius = 0.05 cm; bubble boundary layer thickness = 0.02 cm; influent concentration = 1 g/L; density of aqueous phase = 1 g/mL; viscosity of aqueous phase = 0.01 P; mass transfer rate constant k = 0.0002 cm^2/s ; dt = 10 s; bubble rise velocity = 12.85 cm/s; number of compartments in model (N) = 5 (upper curve), 25 (lower curve).

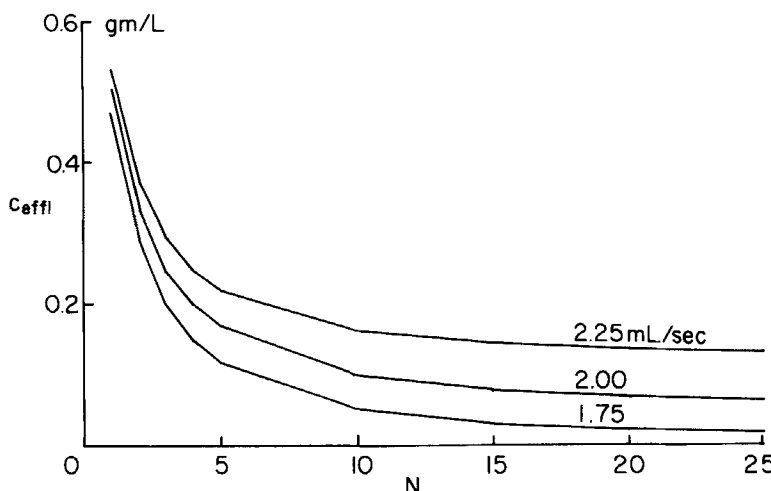


FIG. 4. Steady-state effluent concentrations versus number of compartments used in model. Influent flow rate = 1.75, 2.0, 2.25 mL/s; number of compartments in model (N) plotted on abscissa; other parameters as in Fig. 3.

The time-dependent responses of an aeration column having influent flow rates of 2.5, 2.0, and 1.5 mL/s are shown in Figs. 5, 6, and 7, respectively. The other model parameters are given in the caption to Fig. 5. In each case the lower curve gives the effluent concentration from a column initially charged with water, while the upper curve gives the effluent concentration from a column initially charged with influent. In both cases and at all three flow rates the column has approached steady-state operation in roughly 10^4 s, or 2.8 h. It is apparent that the approach to steady-state conditions is rather sluggish.

Figure 8 shows the responses of an aeration column to time-dependent influent concentrations. In the three runs plotted here the influent concentration, initially 1 g/L, is increased to 5 g/L at 5000 s and held at this value for 1000, 2000, or 3000 s before being reduced back to 1 g/L. The slow response of the effluent concentration to these transient overloads and the prolonged tailing are both consistent with the slow approaches to steady-state conditions seen in Figs. 5-7. This model also readily handles transient variations in the influent flow rate. The ability of the model to deal with such time-dependent input makes it particularly suitable for exploring the behavior of systems which will be used in applications which may involve substantial transient variations, such as waste

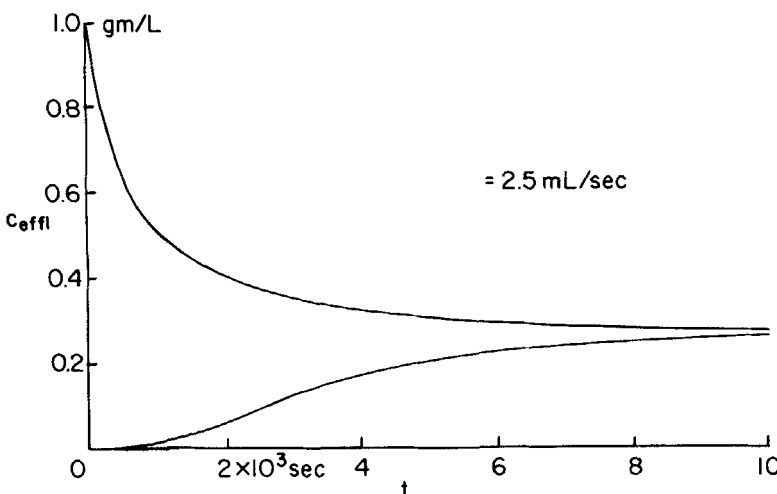


FIG. 5. Approach of effluent concentration to steady state after column start-up. Influent flow rate = 2.5 mL/s; $N = 5$; other parameters as in Fig. 3. The lower curve corresponds to a column initially filled with clean water; the upper, to a column initially filled with influent.

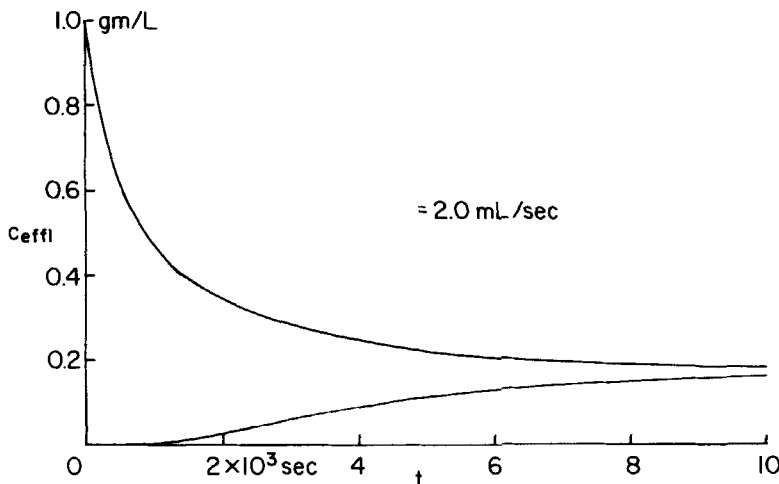


FIG. 6. Approach of effluent concentration to steady state after column start-up. Influent flow rate = 2.0 mL/s; other parameters as in Fig. 5.

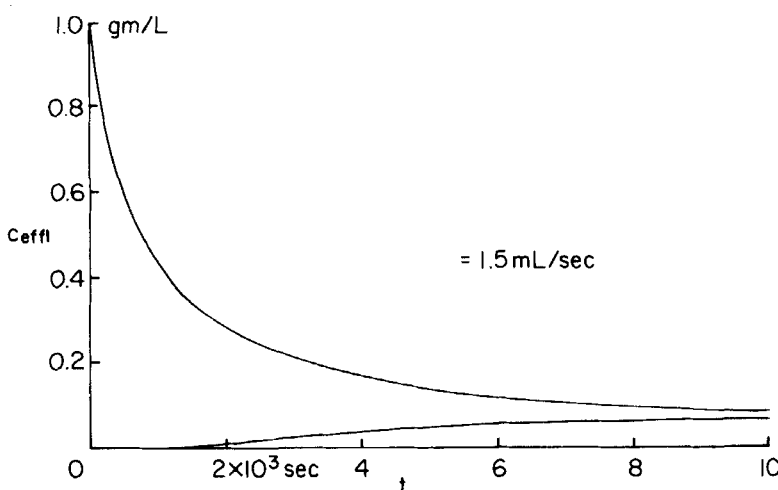


FIG. 7. Approach of effluent concentration to steady state after column start-up. Influent flow rate = 1.5 mL/s; other parameters as in Fig. 5.

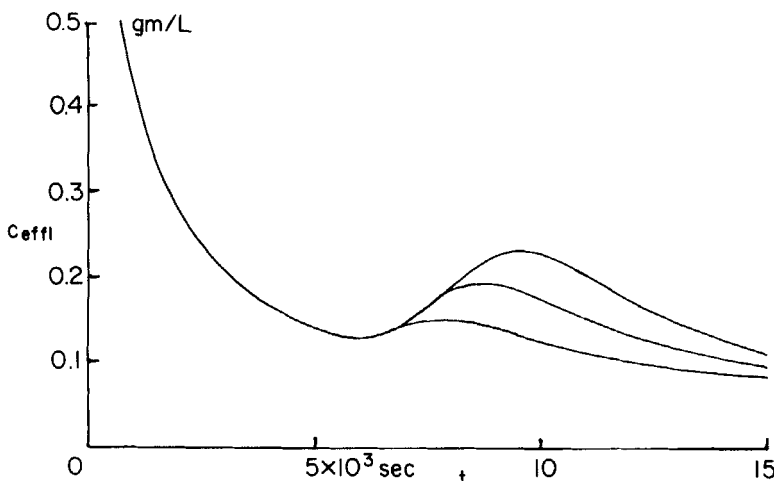


FIG. 8. Effect of influent concentration pulses on column effluent concentration. Influent flow rate = 2.0 mL/s; $N = 5$; initial influent concentration = 1 g/L; influent concentration increases to 5 g/L at 5000 s and is held at this value for 1000 (bottom curve), 2000, and 3000 (top curve) s, after which it returns to 1 g/L. Other parameters as in Fig. 3.

treatment. The dependence of the mass transfer time constant λ_i on the Henry's constant of the solute is illustrated in Fig. 9. It is apparent that, over the range of K_H which one expects for the removal of volatile organic solvents from water, the mass transfer time constant does not vary by much.

The effect of boundary layer thickness, $b - a$, on λ_i , shown in Fig. 10, is quite large. λ_i decreases rapidly with increasing boundary layer thickness, as one would expect. In these runs the bubble radius is held constant. If the bubble radius is varied while the boundary layer thickness is held constant, λ_i varies as illustrated in Fig. 11. The values of λ_i decrease quite rapidly with increasing bubble radius, again as one would expect.

It is generally believed that the boundary layer thickness around a sphere moving in a liquid is of the order of the radius of the sphere (7). We therefore made a set of runs in which the bubble radius and the boundary layer thickness were simultaneously varied, with the boundary layer thickness being set equal to the bubble radius. The results are displayed in Fig. 12, and show that λ_i decreases rapidly with increasing bubble and boundary layer thickness, as expected. Actually, on dimensional grounds one expects that for this set of runs λ_i should vary as the reciprocal of the square of the bubble radius, as is indeed the case.

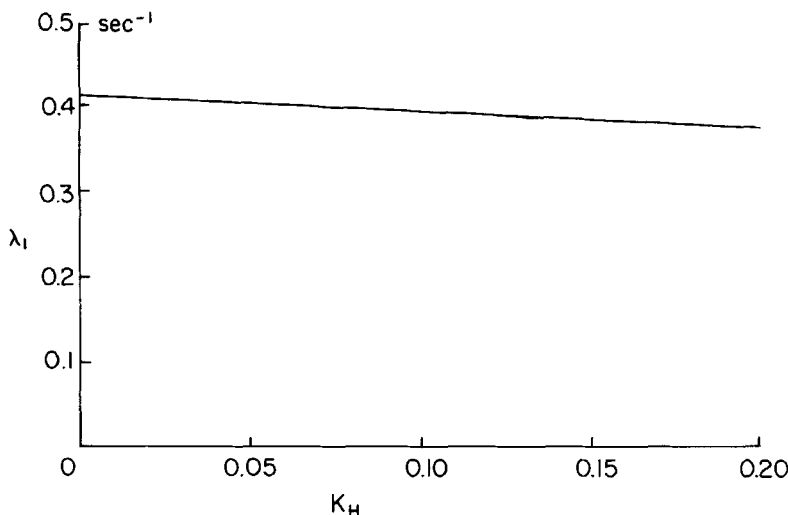


FIG. 9. Dependence of mass transfer rate parameter λ_1 on Henry's constant. Bubble radius = 0.1; boundary layer thickness = 0.1 cm; solute diffusion constant = $0.001 \text{ cm}^2 \cdot \text{s}$.

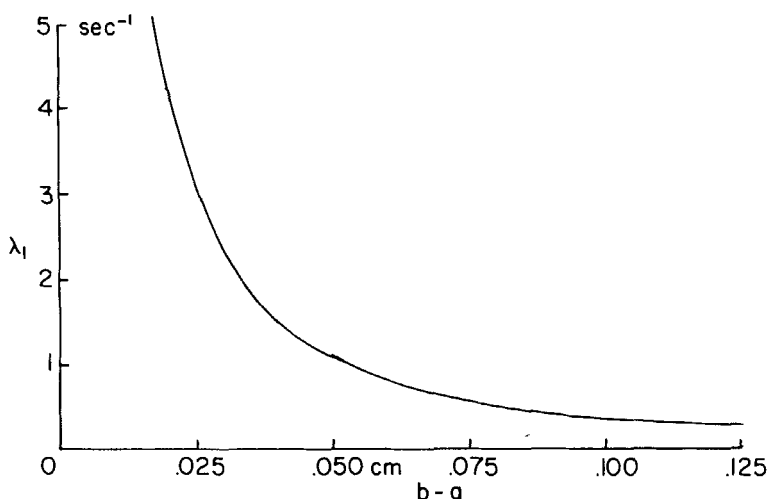


FIG. 10. Dependence of mass transfer rate parameter λ_1 on boundary layer thickness at constant bubble radius. Henry's constant = 0.2 (dimensionless); other parameters as in Fig. 9.

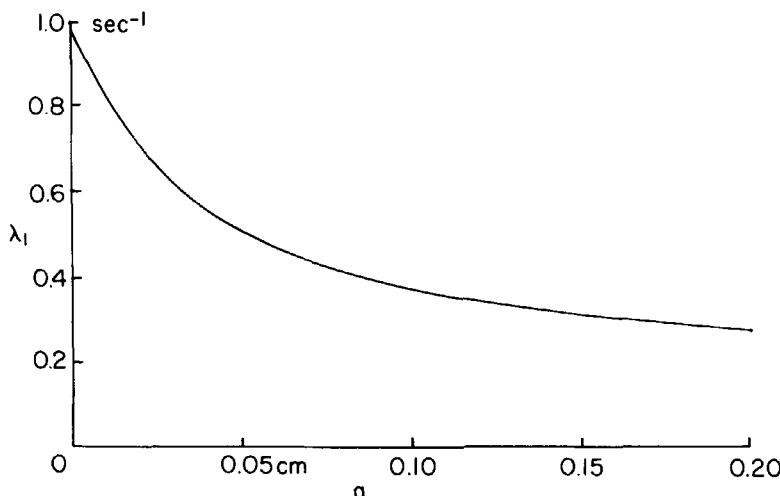


FIG. 11. Dependence of mass transfer rate parameter λ_1 on bubble radius at constant boundary layer thickness. Boundary layer thickness = 0.1 cm; Henry's constant = 0.2; other parameters as in Fig. 9.

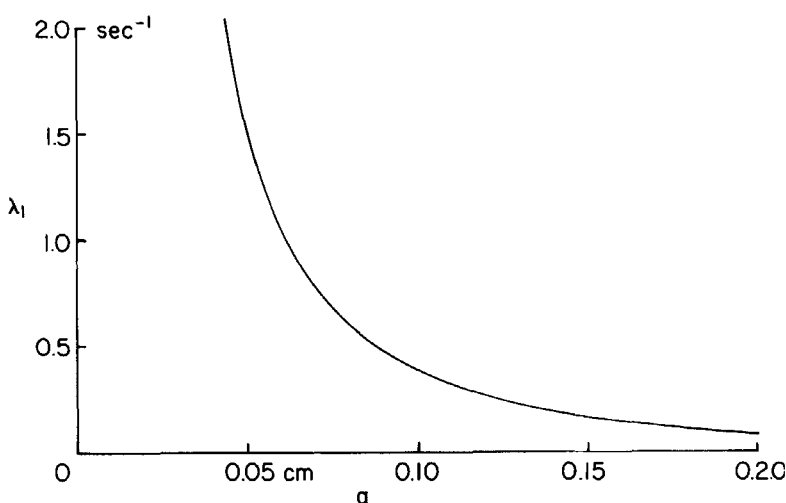


FIG. 12. Dependence of mass transfer rate parameter λ_1 on bubble radius, with boundary layer thickness equal to bubble radius. Henry's constant = 0.2; other parameters as in Fig. 9.

CONCLUSIONS

The time-dependent operation of single- and multistage fine bubble aeration columns with mass transfer kinetics was modeled and the dependence of the results on column parameters was exhibited. Approach of aeration columns to steady-state operation is relatively sluggish, as is their response to concentration pulse overloads. The algorithm used permits the use of relatively large values of Δt , the time increment used in the differential equations modeling a column. This, in turn, permits the modeling of column operation to be readily carried out on commonly available microcomputers. A diskette for computers running MS-DOS which contains the programs for calculating the mass transfer time constant λ_i and for modeling column operation is available from the author at a charge of \$3.00.

Acknowledgement

This work was supported by a grant from the National Science Foundation.

REFERENCES

1. R. E. Treybal, *Mass Transfer Operations*, 2nd ed., McGraw-Hill, New York, 1968.
2. C. J. King, *Separation Processes*, McGraw-Hill, New York, 1971.
3. W. J. Weber Jr., *Physicochemical Processes for Water Quality Control*, Wiley, New York, 1972.
4. G. M. Fair, G. C. Geyer, and D. A. Okun, *Water and Wastewater Engineering*, Vol. 2, Wiley, New York, 1968, Section 25-2.
5. A. Ralston and H. F. Wilf, *Mathematical Methods for Digital Computers*, Wiley, New York, 1960.
6. S.-D. Huang, K. T. Valsaraj, and D. J. Wilson, *Sep. Sci. Technol.*, 18, 941 (1983).
7. H. Schlichting, *Boundary Layer Theory*, McGraw-Hill, New York, 1968.

Received by editor February 1, 1988